FINITE ELEMENT INVESTIGATION ON CFRP-STRENGTHENED BEAM-COLUMN STEEL JOINTS UNDER STATIC AND CYCLIC LOADING

[*1]S. M. Zahurul Islam, [2]S. B. Islam, [3]Md. Tasnimul Hossen Sarker

[1]Department of Civil Engineering, RUET, Bangladesh (zahurul90@gmail.com)
[2]Department of Civil Engineering, RUET, Bangladesh (shariar.islam.ce@gmail.com)
[3]Department of Civil Engineering, RUET, Bangladesh (tasnimul@outlook.com)

***Corresponding Author**

ABSTRACT

In steel structures, interior or exterior beam-column joints like X, T and L- often serve as key load-transferring elements but are particularly susceptible to failure under compressive and cyclic loadings. Carbon Fiber Reinforced Polymer (CFRP) has gained attention as a strengthening material for such elements due to its lightweight nature, high tensile strength, and resistance to corrosion. This study examines the structural enhancement of CFRP-retrofitted steel T-joints subjected to combined compressive and cyclic loading. A numerical investigation was carried out using the finite element software ABAQUS. Eighteen distinct X, T and L-joints configurations, based on varying beam and column cross-sections, were modeled. Model validation was achieved by analyzing non-retrofitted joints under the same load conditions, with results aligning closely with established experimental data. The analysis highlighted a notable increase in load-bearing capacity and crack resistance in joints reinforced with CFRP. Additionally, the load displacement hysteresis curves exhibited improved energy dissipation and stiffness in retrofitted joints. Overall, the study confirms that CFRP retrofitting significantly enhances the mechanical behavior of steel joints. These findings support the use of CFRP as a practical and effective strengthening technique to improve the safety, durability, and performance of steel structures in modern engineering applications.

Keywords: *CFRP; Retrofitting; Finite element analysis; Structural behavior; Tubular section.*

1. INTRODUCTION

Beam-column joints are critical components of steel structures, as they ensure effective transfer of forces between beams and columns. Failure in these joints, particularly under cyclic or seismic loading, can compromise the stability of an entire structural system. To enhance performance and durability, Fiber Reinforced Polymer (FRP) composites, especially Carbon Fiber Reinforced Polymer (CFRP), have emerged as a reliable strengthening solution due to their high tensile strength, lightweight nature, and corrosion resistance (Y. Liu et al., 2020). Several studies have demonstrated the effectiveness of CFRP in retrofitting steel and concrete members. For example, externally bonded CFRP has been shown to improve the cracking resistance of reinforced concrete beams (A. Al-Fakih et al., 2021), while full-scale cyclic tests on CFRP-strengthened circular hollow section (CHS) members confirmed significant improvements in ductility and energy dissipation (T. Tafsirojjaman et al., 2020). CFRP has also been successfully applied to rehabilitate corroded steel pipelines (M. Elchalakani et al., 2017) and to strengthen tubular T-joints under axial loading, improving both load capacity and failure modes (M. Lesani et al., 2014). Beyond metallic joints, recent investigations on non-metallic GFRP T-joints (T. M. Higgoda et al., 2023) and offshore steel tubular joints (A. Sadat Hosseini et al., 2019) further highlight the potential of FRP in critical structural applications. Other strengthening approaches, such as reinforcement of hollow section joints with internal stiffeners, have also been explored to delay local failure and enhance capacity (H. Chang et al., 2018). Numerical research has extended this understanding by examining CFRP retrofitted steel members under transverse impact (M. I. Alam et al., 2015) and adhesively bonded T-joints with structural sandwiches (S. M. R. Khalili et al., 2011). Despite these advances, limited studies have focused on the finite element modeling of CFRP-strengthened beam-column steel T-joints under both static and cyclic loading. This paper addresses this gap by developing a detailed FE model to evaluate the structural response, load-carrying capacity, and energy dissipation of CFRP-retrofitted joints, aiming to offer practical insights for strengthening deficient steel structures.

2. MATERIALS AND METHODOLOGY

Specimens used in this test were of varying dimensions. Full-scale interior joints (X) and exterior joints (T and L) and small-scale T joints were modeled for axial and cyclic loading simulation. Fig. 1 and Table 2 demonstrate the properties and dimensions of the specimen materials. The numerical analysis utilized CFRP with a fiber strength of 4900 MPa, fiber stiffness of 230 GPa, and fabric thickness of 0.1 mm. The adhesive qualities of the material are characterized by a tensile strength of 49.8 MPa and a shear strength of 29 MPa. The properties listed above were derived from cited papers [18], [19]. Finite Element Analysis (FEA) faces difficulty in simulating beam-column steel joint strengthening with CFRP due to complications like welded connections and material interactions. Deformation patterns and ultimate strength depend on steel and CFRP characteristics. Realistic modeling pays attention to each component. Nine steel joint models- square sections, I-sections, and circular sections were used, representing the beam and column composite shell for CFRP. Specimen dimensions have been chosen depending on local market availability for practical alignment.

Table 1: Properties of Steel

Density	7,850 kg/m^3 (0.284 lb/in^3)
Young's Modulus	200 GPa (29,000 ksi)
Poisson's ratio	0.3
Yield Stress	367.9 N/mm^2
Yield Strain	0.00171 mm/mm

Table 2: Specimen Dimension for FEA Model

Model	Specimen material	Dimension (mm)	
		Full scale	Small scale
Square Section	Mild Steel	300 × 300 × 6	100 × 100 × 3
I-Section		180 × 300 × 6	100 × 100 × 3
Circular Section		300 × 6	100 × 3

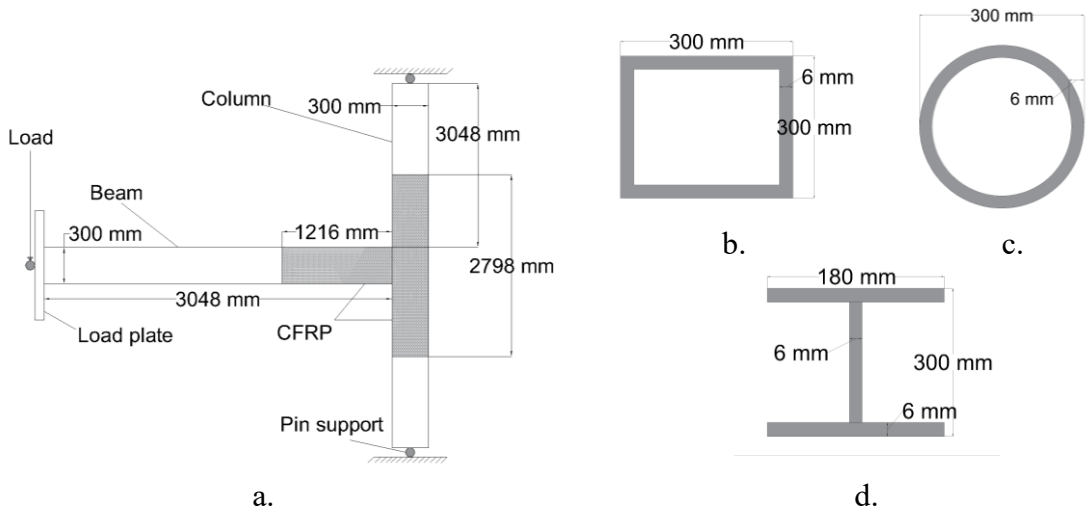

Figure 1: Dimensions of Full-Scale Specimens (a) T joint, (b) Square-section, (c) Circular-section, (d) I-section

3. NUMERICAL MODELING

To investigate the structural behavior of beam-column steel joints reinforced with CFRP, finite element models were prepared using Abaqus software. In the joint core and CFRP-bonded areas, where high stress gradients and localized deformation were anticipated, special attention was paid to mesh refinement. Under axial and cyclic loading conditions, the modeling approach tried to accurately replicate load transfer mechanisms, stress distribution, and deformation characteristics. Figure 2 shows the finite element configurations used for various joint types.

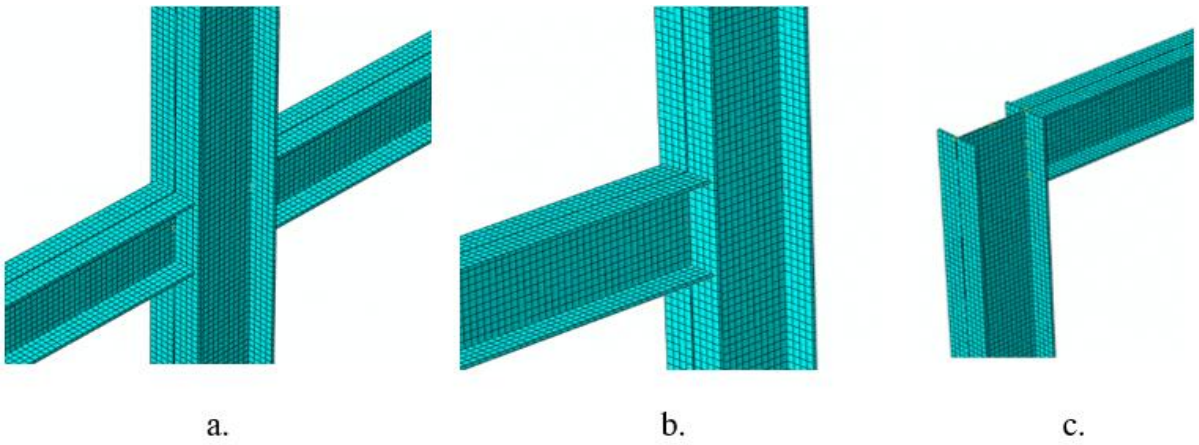

Figure 2: FE Models Used for Different Beam-Column Joints of I- section (a) X, (b) T & (c) L Joints

The FE software Abaqus was utilized to systematically analyze the CFRP-retrofitted joints due to its excellent nonlinear analysis functionality. The tubular members were modeled using solid element C3D8R with reduced integration. This element in particular has the ability to avoid shear self-locking and achieve convergence despite serious element distortions. The CFRP sheets were modeled using membrane-type element M3D4R because this element only has in-plane stiffness, similar to the mechanical characteristics of CFRP. To simplify the FE analysis, it was assumed that relative slipping did not occur between tubular members and the CFRP sheet; therefore, they were connected using the *TIE constraint. FE models of three different types of joints using steel I-section with meshing are shown in Figure 2. To obtain accurate results with reasonable calculation costs, the regions where the CFRP and the chord were in contact with each other and the portion of the brace near the joint were fine-meshed, while the mesh was coarser further away from these interaction regions. Finally, please note that the numerical analysis model ignored the effects of factors such as welding and geometric defects.

4. NUMERICAL RESULTS AND DISCUSSION

4.1 Experimental Validation

In this study, validation was achieved by comparing the numerically predicted outcomes to experimental results obtained from previous research. Figure 3 shows an ultimate load carrying capacity of 40.5 kN for experimental specimen, while the numerical model projected a load of 42.33 kN at without CFRP condition. Around 4.5% variation observed between experimental and numerical data.

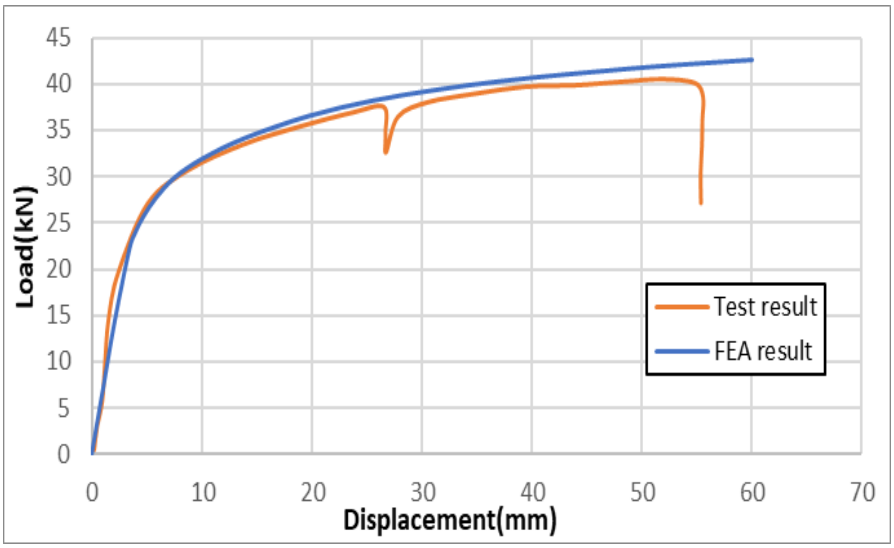

Figure 3: Comparison between Experimental and Numerical Results of I-section

4.2 Full Scale Beam-Column Joint under Axial Load

After the numerical model was successfully validated, a parametric study was performed on full-scale beam-column joints under monotonic axial loading. The analysis examined nine joint configurations, including X-, T-, and L-type connections featuring I-section, square-section, and circular-section members, assessed both with and without CFRP reinforcement. The main goal was to look at how stress builds up, how loads move through the system, and how CFRP confinement affects joint behavior. Stress contour distributions derived from finite element simulations illustrate critical stress concentration zones and the ability of CFRP retrofitting in mitigating localized damage. Figure 4 shows stress contours that are typical for the joints that haven't been strengthened by CFRP.

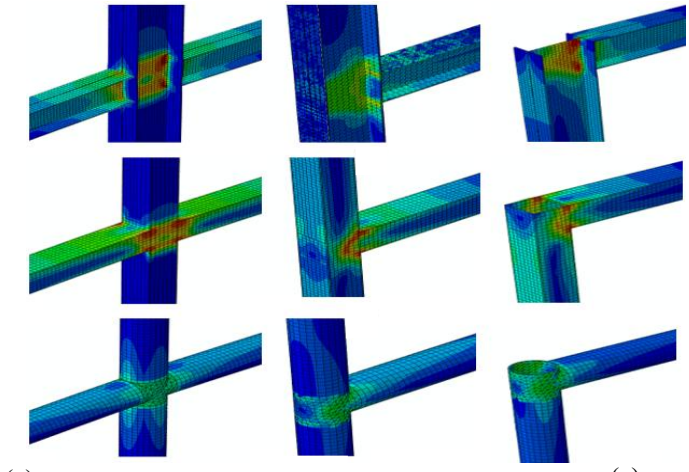

(a) (b) (c)

Figure 4: Representation of Stress Distribution for Non-Strengthened Joints of (a) I-sections, (b) Square-sections & (c) Circular-sections

The load-displacement responses of the full-scale joints were compared for strengthened and unstrengthen conditions in order to quantitatively evaluate the efficiency of CFRP strengthening. The findings show that different joint types and cross-sections have different initial cracking loads, ultimate load capacities, and overall stiffness. Figure 5 presents these responses under axial loading in a comparative manner. At Figure 5(a) using a downward vertical displacement of u=90 mm, the initial cracking load of the non-retrofitted model is 158.33 kN for X joint, 131.89 kN for T joint and 113.28 kN for L joint. Whereas the ultimate load capacity of the retrofitted model reaches 182.54 kN, 170.24 kN and 148.90 kN for X, T and L joints respectively. Representing an increase of approximately 15.30%, 29.07% and 31.44% compared to the unstrengthened model. Similarly in Figure 5(b) under an applied displacement of 30mm, the initial cracking load of the retrofitted model is 115.02 kN for X joint, 111.46 kN for T joint and 103.661kN for L joint. Whereas the ultimate load capacity of the retrofitted model reaches 128.40 kN, 122.01 kN and 107.35 kN for X, T and L joints respectively. Representing an increase of approximately 21.73%, 19.39% and 12.63% compared to the unstrengthened model. And lastly in Figure 5(c) under an applied displacement of 90mm Under an applied displacement of 90mm, the initial cracking load of the retrofitted model is 97.65 kN for X joint 94.25 kN for T joint and 90.78 kN for L joint. Whereas the ultimate load capacity of the retrofitted model reaches 103.08 kN, 98.28 kN and 93.09 kN for X, T and L joints respectively. Representing an increase of approximately 12.65%, 18.64% and 10.07% compared to the unstrengthened model.

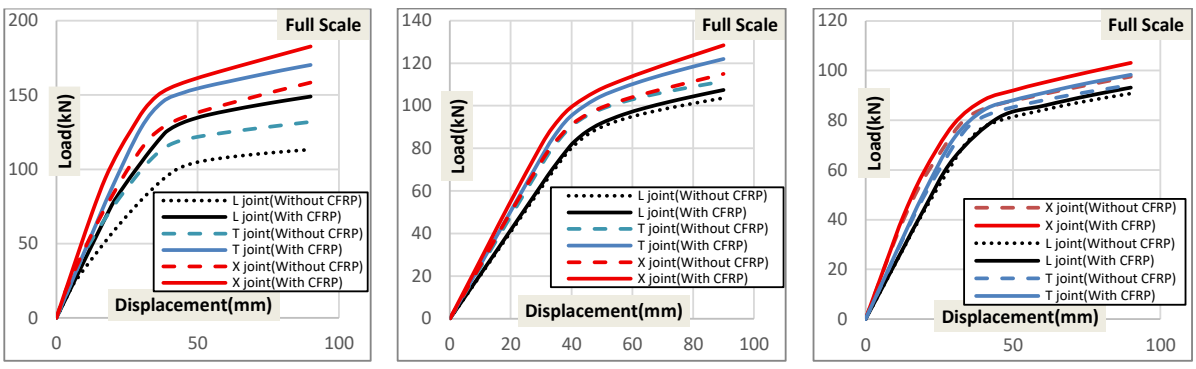

a. b. c.

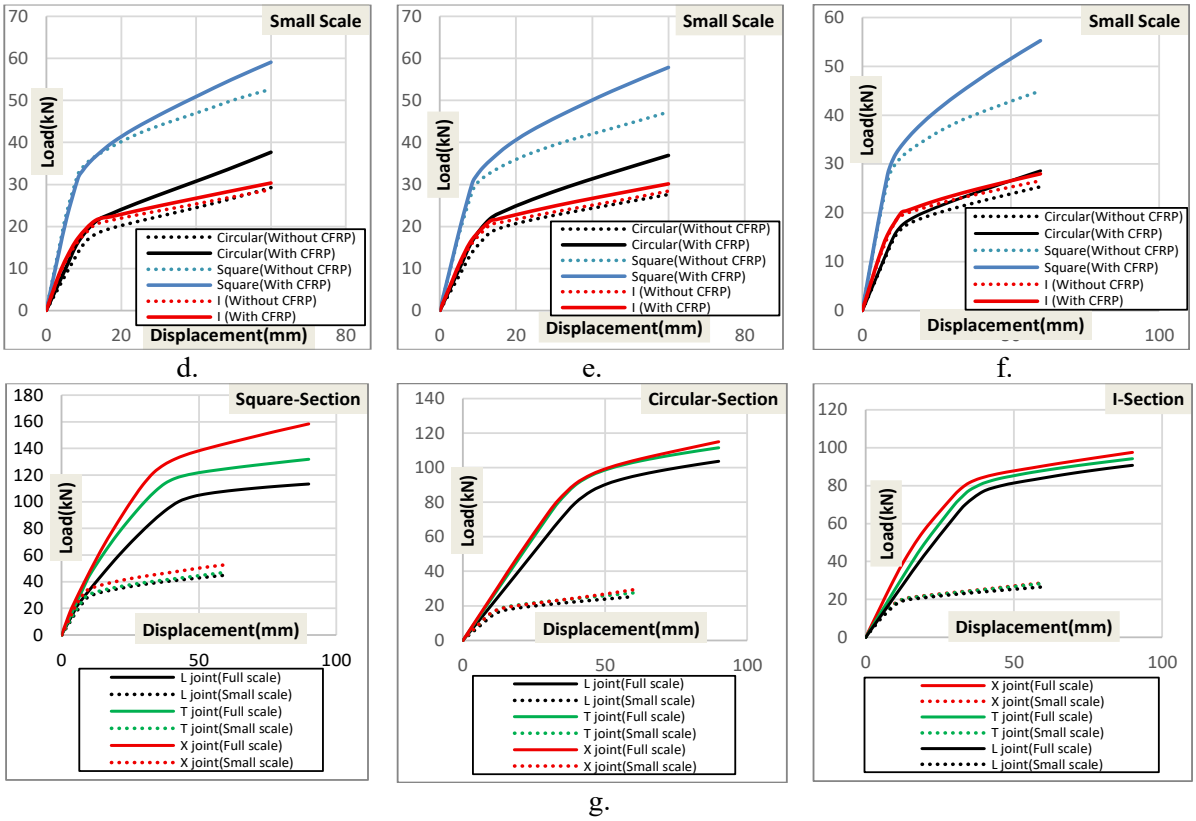

Figure 5: Comparison of Load-Displacement Performance between CFRP Strengthened and Non-strengthened Section (a) Square, (b) Circular, (c) I (d) X, (e) T (f) L-Joints and (g) Comparison between Full-scale and Small-scale specimen results under axial load

4.3 Small Scale Beam-Column Joint under Axial Loading

After simulating the full-scale specimens, nine relatively small sized consecutive specimens were also modeled, and axial and cyclic loading analysis was conducted. Here the displacement found under load was also less compared to the full-scale models which was u=60 mm for circular, square and I-section. Here all the joints were considered for analysis, both with and without CFRP. Figures 5(d), 5(e) and 5(f) show the variation of performance of these specimens under the same axial load.

4.4 Cyclic Load Simulation of Small Scale Beam-Column Joint

Under cyclic loading, unstrengthened joints demonstrated significant stiffness degradation and accumulated plastic deformation over successive load cycles. The stiffness remained more stable over the loading cycles, and residual deformation after unloading was substantially reduced. This was due to the confinement provided by CFRP wraps, which limited the plastic strain and delayed crack initiation. The energy dissipation capacity, a key indicator of seismic performance, increased noticeably in CFRP-retrofitted joints. The area under the load-displacement hysteresis curves was significantly larger compared to the bare joint, indicating better ductility and energy absorption.

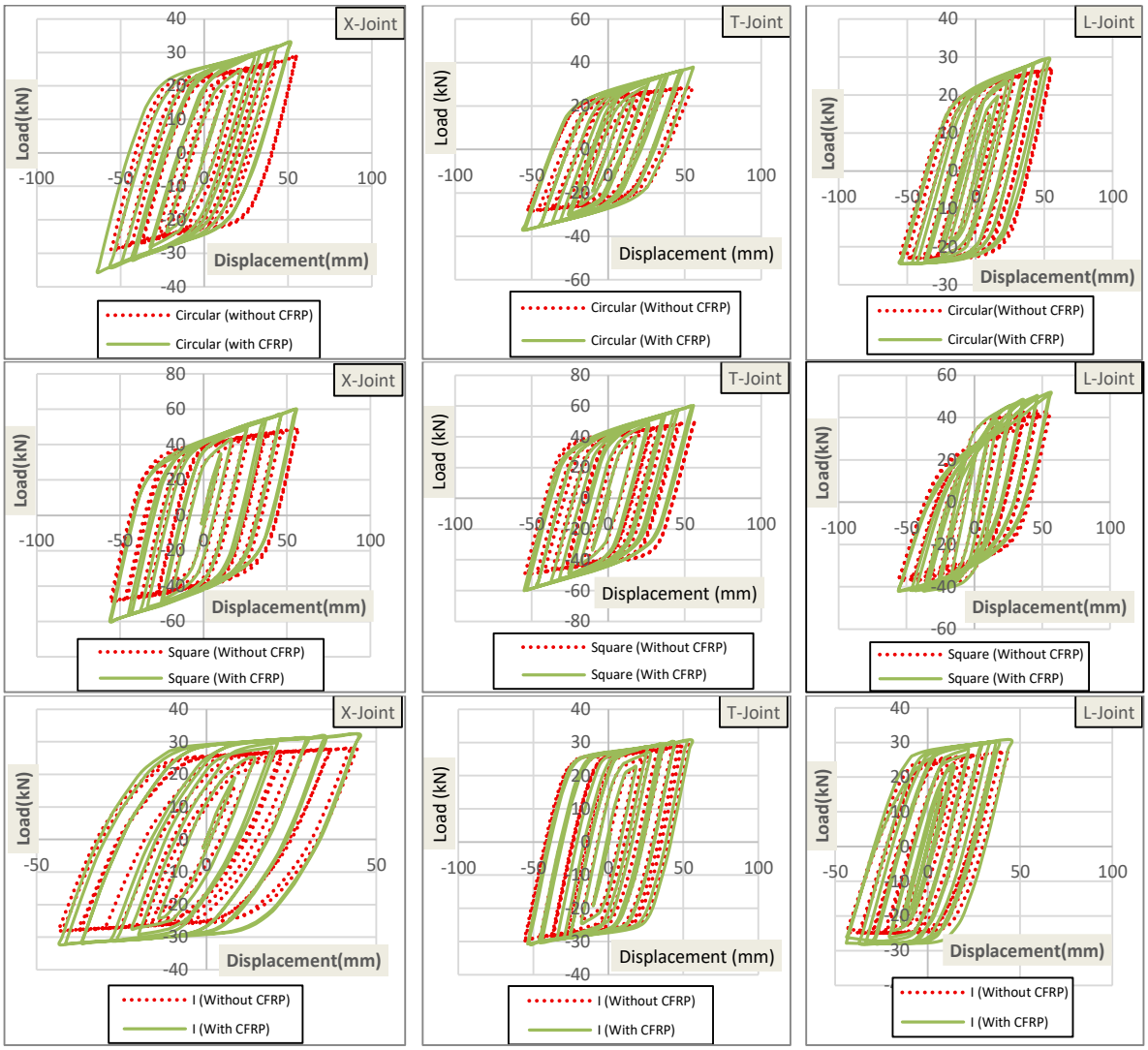

Figure 6: Hysteresis Curves of CFRP Strengthened and Non-strengthened Small-scale Different Joints under Cyclic Load

Additionally, the strength degradation rate per cycle was slower in the CFRP-strengthened one. Figure 6 represents all the variations of performance of different joints with different cross sections under the same amount cyclic loading. Here in Figure 7, the backbone curves represent that Square section carries more load than the circular and I sections and it is certain because of the more cross-section area and flat face gives efficient load transfer.

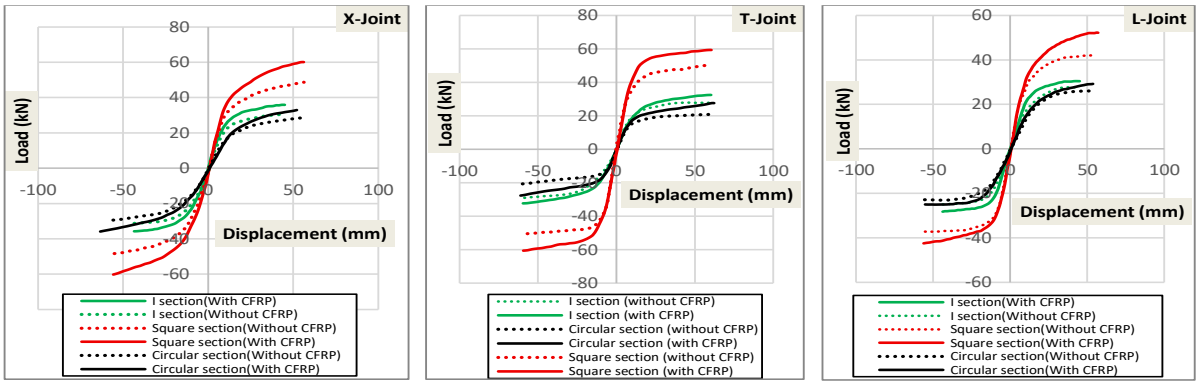

Figure 7: Comparison between Backbone Curves of Different Small-scale Joints under Cyclic Load

The ultimate load carrying capacity between circular and I sections were very close. Though the curve in the yield region was steeper in the I-sections. Besides it was also noticed that the effect of CFRP was more in the square section joints than the other two and the least was in the I-section. In number which is on average 22.07%. Whereas the improvement in circular and I-section was on average 13.2%.

5. CONCLUSION

This study presented a comprehensive finite element investigation on the structural behavior of CFRP-strengthened beam-column steel joints subjected to axial and cyclic loading. A thorough parametric analysis covering various joint configurations and cross-sectional geometries were conducted after the numerical modeling approach was first verified against available experimental results to ensure reliability. The main conclusions of this study are summed up as follows based on the numerical results from both full-scale and small-scale models.

Experimental validation shows around 4.5% variation between experimental and numerical data. I-section joints under axial loading exhibit increase of approximately 15.65%, 14.30% and 13.07% compared to the unstrengthened model for X, T and L joints respectively. Similarly square section joints under axial loading exhibit increase of approximately 22.7%, 21.20% and 21.44%. And lastly the circular section joints exhibit increase of 33.21%, 32.69% and 9.21% compared to the unstrengthened model for X, T and L joints respectively. So, the strengthing effect was seen more in the circular section joints, specially in X-joints. Under cyclic loading, square-section joints showed significantly higher load capacities with higher energy dissipation after CFRP strengthening, marking a 23.28% increase in positive vertical displacement and almost 22.07% increase in negative displacement. Similarly, I-section T-joints under cyclic loading exhibit notable load capacity increases with CFRP strengthening, with a 17.86% increase in positive displacement and 19.39% increase in negative displacement and circular-section T-joints under cyclic loading exhibit notable load capacity increases with CFRP strengthening with a 15.84% increase in positive displacement and 12.42% in negative displacement.

Among the 3 joints, maximum load carrying capacity was observed in the interior x joint and the lowest was in the exterior L-joint. Above all, the hysteresis results showed that, under cyclic loading, CFRP-reinforced T-joints are better at carrying loads and dissipating energy than bare metal joints. From Fig. 5(g), it becomes clear that although the overall behavioral trends are quite similar in both scales, there is a noticeable difference in the magnitude of load-carrying capacity. Specifically, the full scale models exhibit a significant increase in ultimate load compared to their small-scale counterparts. Despite this, the relative order of performance between the sections remain consistent.

ACKNOWLEDGEMENT

The authors gratefully have acknowledged the financial support of the University Grants Commission of Bangladesh under the Project No.: DRE/08/RUET/764(52)/Pro/2025-2026/01.

REFERENCES

Y. Liu, T. Tafsirojjaman, A. U. R. Dogar, and A. Hückler, “Shrinkage behavior enhancement of infra-lightweight concrete through FRP grid reinforcement and development of their shrinkage prediction models,” Constr Build Mater, vol. 258, Oct. 2020, doi: 10.1016/j.conbuildmat.2020.119649

T. Tafsirojjaman, S. Fawzia, and D. Thambiratnam, “Investigation on the behaviour of CFRP strengthened CHS members under monotonic loading through finite element modelling,” Structures, vol. 28, pp. 297–308, Dec. 2020, doi: 10.1016/j.istruc.2020.08.059

A. Al-Fakih, M. Hisbany Mohd Hashim, R. Alyousef, A. Mutafi, S. Hussein Abo Sabah, and T. Tafsirojjaman, “Cracking behavior of sea sand RC beam bonded externally with CFRP plate,” Structures, vol. 33, pp. 1578–1589, Oct. 2021, doi: 10.1016/j.istruc.2021.05.042

T. Tafsirojjaman, S. Fawzia, D. P. Thambiratnam, and X. L. Zhao, "Study on the cyclic bending behaviour of CFRP strengthened full-scale CHS members," Structures, vol. 28, pp. 741–756, Dec. 2020, doi: 10.1016/j.istruc.2020.09.015

M. Elchalakani, A. Karrech, H. Basarir, M. F. Hassanein, and S. Fawzia, "CFRP strengthening and rehabilitation of corroded steel pipelines under direct indentation," Thin-Walled Structures, vol. 119, pp. 510–521, Oct. 2017, doi: 10.1016/j.tws.2017.06.013

M. Lesani, M. R. Bahaari, and M. M. Shokrieh, "Experimental investigation of FRP-strengthened tubular T-joints. under axial compressive loads," Constr Build Mater, vol. 53, pp. 243–252, Feb. 2014, doi: 10.1016/j.conbuildmat.2013.11.097

T. M. Higgoda, M. Elchalakani, M. Kimiaei, B. Yang, and X. Guo, "Experimental investigation on the structural behaviour of novel non-metallic pultruded circular tubular GFRP T-joints under axial compression," Thin-Walled Structures, vol. 184, p. 110512, 2023, doi: https://doi.org/10.1016/j.tws. 2022.110512

A. Sadat Hosseini, M. R. Bahaari, and M. Lesani, "Stress concentration factors in FRP-strengthened offshore steel tubular T-joints under various brace loadings," Structures, vol. 20, pp. 779–793, Aug. 2019, doi: 10.1016/j.istruc.2019.07.004

H. Chang, J. Xia, Z. Guo, C. Hou, W. Din, and F. Qin, "Experimental study on the axial compressive strength of vertical inner plate reinforced square hollow section

M. I. Alam and S. Fawzia, "Numerical studies on CFRP strengthened steel columns under transverse impact,"Compos Struct, vol. 120, pp. 428–441, Feb. 2015, doi: 10.1016/j.compstruct.2014.10.022

S. M. R. Khalili and A. Ghaznavi, "Numerical analysis of adhesively bonded T-joints with structural sandwiches and study of design parameters," Int J Adhes Adhes, vol. 31, no. 5, pp. 347–356, Jul. 2011, doi: 10.1016/j.ijadhadh.2010.12.005